# MoTaDual: Modality-Task Dual Alignment for Enhanced Zero-shot Composed Image Retrieval

# Haiwen Li<sup>1</sup> Fei Su<sup>1,2</sup> Zhicheng Zhao<sup>1,2</sup>

<sup>1</sup>Beijing University of Posts and Telecommunications
<sup>2</sup>Beijing Key Laboratory of Network System and Network Culture, China {lihaiwen, sufei, zhaozc}@bupt.edu.cn

#### **Abstract**

Composed Image Retrieval (CIR) is a challenging visionlanguage task, utilizing bi-modal (image+text) queries to retrieve target images. Despite the impressive performance of supervised CIR, the dependence on costly, manually-labeled triplets limits its scalability and zero-shot capability. To address this issue, zero-shot composed image retrieval (ZS-CIR) is presented along with projection-based approaches. However, such methods face two major problems, i.e., task discrepancy between pre-training (image ↔ text) and inference (image+text → image), and modality discrepancy. The latter pertains to approaches based on text-only projection training due to the necessity of feature extraction from the reference image during inference. In this paper, we propose a two-stage framework to tackle both discrepancies. First, to ensure efficiency and scalability, a textual inversion network is pre-trained on large-scale caption datasets. Subsequently, we put forward **Mo**dality-**Ta**sk **Dual** Alignment (MoTaDual) as the second stage, where large-language models (LLMs) generate triplet data for fine-tuning, and additionally, prompt learning is introduced in a multi-modal context to effectively alleviate both modality and task discrepancies. The experimental results show that our MoTaDual achieves the state-ofthe-art (SOTA) performance across four widely used ZS-CIR benchmarks, while maintaining low training time and computational cost. The code will be released soon.

# 1 Introduction

Composed Image Retrieval (CIR) (Vo et al. 2019; Baldrati et al. 2022) focuses on retrieving target images that align closely with a reference image while incorporating specified textual modifications. This approach leverages bi-modal queries, combining visual and textual inputs to enable users to perform more precise and flexible searches. Recently, the increasing availability of pre-training image-text models (Radford et al. 2021; Jia et al. 2021; Li et al. 2021) has spurred interest in CIR for practical applications, particularly in e-commerce and online search. Supervised CIR methods (Vo et al. 2019; Baldrati et al. 2022) utilize labeled triplets  $(I_r, T_c, I_t)$ , where  $I_r$  represents the reference image,  $T_c$  denotes the textual modification, and  $I_t$  is the target image. However, obtaining sufficient labeled triplets is challenging due to the labor-intensive and time-consuming manual annotations (Liu et al. 2021; Wu et al. 2021), resulting in smaller datasets that limit the generalization ability.

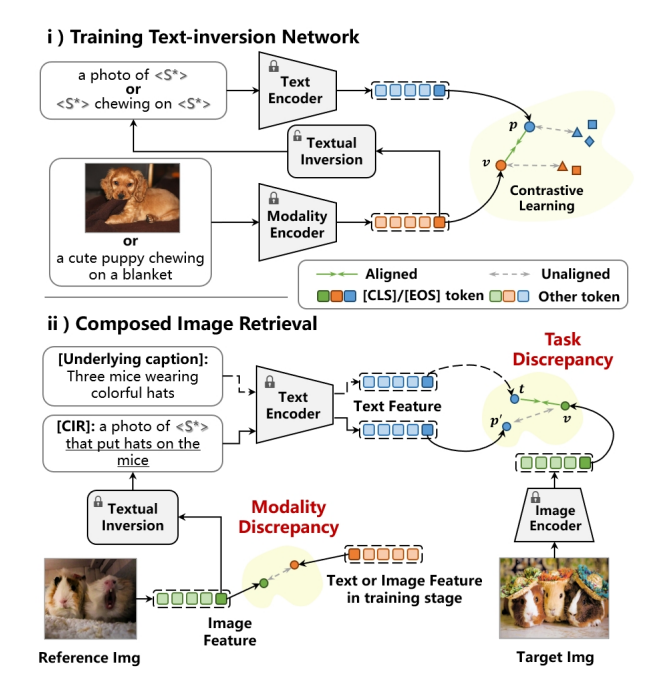


Figure 1: **Projection-based approaches for ZS-CIR.** (i) Pic2Word (Saito et al. 2023) and SEARLE (Baldrati et al. 2023) use the features obtained from the image encoder as inputs to the textual inversion network for contrastive training, whereas Lincir (Gu et al. 2024b) employs text-only training. (ii) Task discrepancy (Byun et al. 2024) is encountered during inference. Additionally, Lincir also faces modality discrepancy.

Instead of relying heavily on pre-collected triplet datasets, Zero-shot Composed Image Retrieval (ZS-CIR) (Saito et al. 2023; Baldrati et al. 2023; Gu et al. 2024b) has emerged as a scalable solution to overcome the limitations of supervised CIR. Compared to CIR, ZS-CIR can harness significantly larger and more diverse publicly available datasets that encompass a broader range of domains and semantic categories. Specifically, the training datasets for CIR typically comprise tens of thousands of samples, such as FashionIQ (Wu et al. 2021) with approximately 47k samples, while CIRR (Liu et al. 2021) has a size of around 29k. In

contrast, ZS-CIR leverages datasets that scale up to millions or even billions for training, e.g., Laion-5b (Schuhmann et al. 2022), CC3M (Sharma et al. 2018), thereby equipping the models with enhanced zero-shot capabilities.

The main problem faced by ZS-CIR is how to effectively combine textual and visual features to establish a comprehensive query for retrieving. To address this issue, projection-based approaches have been proposed. As illustrated in Figure 1(i), Pic2Word (Saito et al. 2023) and SEARLE (Baldrati et al. 2023) utilize a textual inversion network (Cohen et al. 2022; Gal et al. 2022) to project the input image feature into the token embedding space. The projected feature is then concatenated with other text tokens and fed into the text encoder, leveraging the ability of text encoder to flexibly integrate information from the input token sequence. Another notable work (Gu et al. 2024b) eliminates the use of image encoder and relies solely on text-based projection training, dramatically reducing resource consumption during training and achieves even superior performance.

However, the projection-based methods have two major issues, as shown in Figure 1(ii). The first issue, task discrepancy, arises because the training stage only involves mapping image or text features to a specific token, denoted as <S\*>, without feature combination and target retrieval. Afterwards, zero-shot inference is directly performed with the template prompt "a photo of  $\langle S \star \rangle$  that  $T_c$ " to retrieve the target image, which is inadequate. From a different perspective, Vision-Language Pretraining (VLP) models like CLIP are pre-trained by image-text matching. As a result, assuming the existence of an underlying caption for the target image, the projection-based methods often struggle to fit this caption during the inference stage. The second issue, modality discrepancy, pertains to methods like Lincir (Gu et al. 2024b) that adopt text-only training to improve efficiency and scalability. However, the main drawback is that during inference, they must extract features from the reference image, which results in modality discrepancy.

To tackle these problems, we present a two-stage training framework. First, we pre-train a textual inversion network. Considering efficiency and scalability, we opt for the textonly training approach (Gu et al. 2024b). Furthermore, we introduce a second stage of fine-tuning, dubbed as MoTaDual (Modality-Task Dual Alignment), to address the task and modality discrepancies. Unlike existing methods only utilizing text triplets (Byun et al. 2024; Gu et al. 2024b), the dataset used by MoTaDual includes reference images to perform both modality alignment and task adaption. Due to the image-text matching nature of CLIP (Radford et al. 2021), the target can be either in image or text modality. Since target images are not easily obtainable, we adopt triplets in the form of  $(I_r, T_c, T_t)$  for fine-tuning, where  $I_r$  represents the reference image with caption  $T_r$ . With well-crafted prompts, large-language models (LLMs) can easily generate the textual modification  $T_c$  and target text  $T_t$  based on  $T_r$ . Another issue is how to fine-tune the model, as simply fine-tuning the entire text and image encoders or parts of their parameters certainly demands substantial computational cost. Therefore, we adopt prompt tuning (Zhou et al. 2022b,a; Khattak et al. 2023), which involves inserting only a few learnable

vectors, thereby ensuring highly parameter-efficient. Additionally, since fine-tuning both encoders is necessary, we introduce a multi-modal prompt tuning method inspired by MaPLe (Khattak et al. 2023).

In summary, our contributions are threefold:

- We propose a two-stage training framework. First, a textual inversion network is pre-trained on large-scale caption datasets. Then, Modality-Task Dual Alignment (Mo-TaDual) is presented, where LLMs generate new triplet data for fine-tuning.
- We introduce prompt tuning to ZS-CIR and utilize it for fine-tuning in a multi-modal context to address modality and task discrepancies. To the best of our knowledge, this is the first application of prompt tuning in ZS-CIR.
- Compared to the strong baseline (Gu et al. 2024b), Mo-TaDual further enhances retrieval performance by a large margin across four widely-used ZS-CIR datasets, while maintaining low training time and computational cost.

#### 2 Related Work

Composed Image Retrieval. Composed Image Retrieval (CIR) (Vo et al. 2019; Anwaar, Labintcev, and Kleinsteuber 2021; Kim et al. 2021; Baldrati et al. 2022; Xu et al. 2024), aims to retrieve target images that have been textually modified, based on a given reference image. To this end, an autoencoder-based method, ComposeAE (Anwaar, Labintcey, and Kleinsteuber 2021), is proposed to learn the composition of image and text features. Another line of work is the recent state-of-the-art method CLIP4Cir (Baldrati et al. 2022), which fine-tunes a CLIP text encoder but still remains dependent on annotated triplets. Recent research has introduced zero-shot composed image retrieval (ZS-CIR), which does not require manually annotated triplets for training. Representative methods combine image and text features into a single query for retrieval using a textual inversion network (Gal et al. 2022), including image-based Pic2Word (Saito et al. 2023) and SEARLE (Baldrati et al. 2023), and text-based approach Lincir (Gu et al. 2024b). Additionally, some attempts (Byun et al. 2024; Tang et al. 2024; Suo et al. 2024) have improved upon textual inversion training, such as ContextI2W (Tang et al. 2024), which introduces two complementary modules that collaboratively map an image to a context-dependent pseudo-word token without additional supervision. Most related to ours is RTD (Byun et al. 2024) that tackles the task discrepancy. However, we go further by addressing modality discrepancy and, unlike full or partial fine-tuning in RTD, we adopt prompt tuning to markedly reduce the computational complexity.

**Prompt Tuning.** A prompt, serving as an instruction input to VLP models, is used to enhance its understanding of the task. Prompts can either be manually crafted or automatically learned. The latter is known as prompt tuning, initially introduced by the Natural Language Processing (NLP) (Lester, Al-Rfou, and Constant 2021; Li and Liang 2021), achieveing performance comparable to full fine-tuning. Prompt tuning is later adapted to Computer Vision (CV) and Multi-modal Learning (MML). For instance, VP (Bahng et al. 2022) and VPT (Jia et al. 2022) insert a

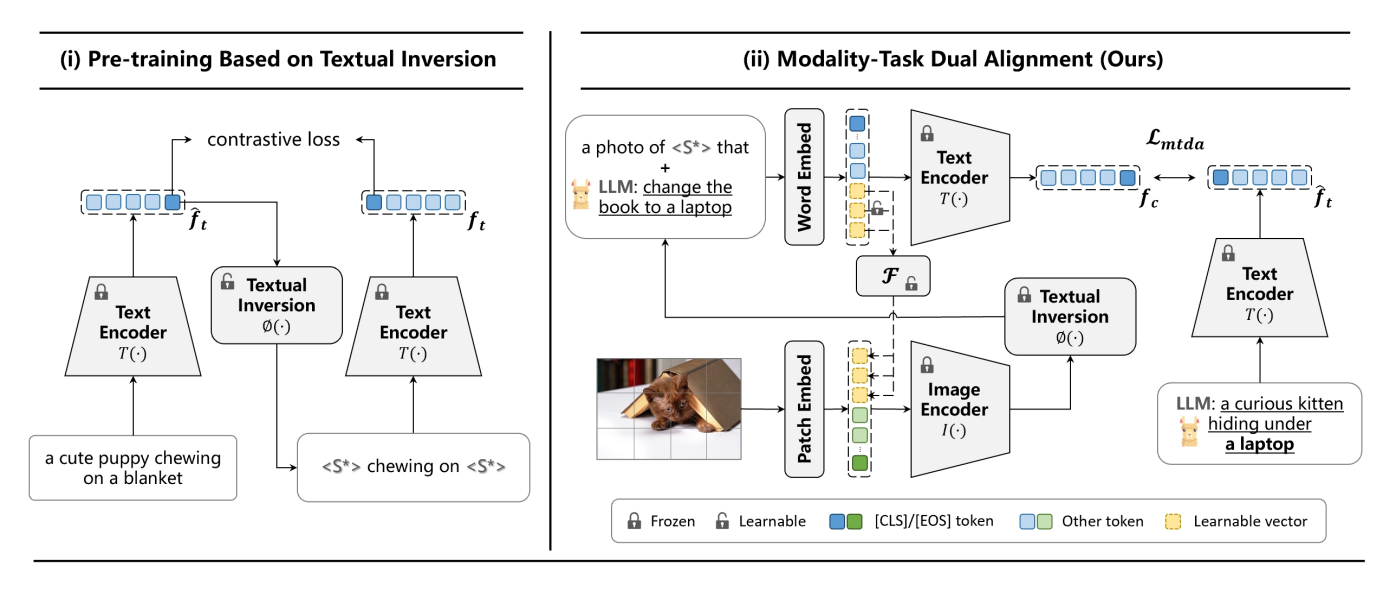


Figure 2: **Overview of our training framework.** (i) The first stage efficiently trains a textual inversion network  $\phi$  with only caption data. (ii) Modality-Task Dual Alignment: We employ multi-modal prompt tuning by inserting a few learnable vectors on the text side, which are then transformed to the image side via a coupling function  $\mathcal{F}$ . The dual encoder is then jointly tuned using the triplets generated by LLMs, effectively mitigate both task and modality discrepancies.

small amount of learnable parameters into the image encoder to adapt it to downstream tasks, while CoOp (Zhou et al. 2022b) and CoCoOp (Zhou et al. 2022a) introduce a few trainable vectors on the text side of CLIP (Radford et al. 2021), achieving excellent effects. Recently, Fang et al. deploy prompt tuning to cross-domain retrieval, revealing its feasibility in complex retrieval scenarios. In addition, MaPLe (Khattak et al. 2023) presents multi-modal prompt learning, inserting trainable vectors on the text side and transferring them to the vision side through a coupling function for joint tuning.

## 3 Methodology

In this section, we describe our MoTaDual for ZS-CIR, which follows a general two-stage framework as shown in Figure 2. Considering the efficiency and scalability of text-only training (Gu et al. 2024b), we first pre-train a textual inversion network  $\phi$  on caption datasets. To simultaneously address task and modality discrepancies, we subsequently freeze  $\phi$  and fine-tune the dual encoder by multi-modal prompt learning on triplet data generated by LLMs.

#### 3.1 Generation of Triplet Data Based on LLMs

Since supervised CIR heavily relies on labor-intensive manual annotation of triplets  $(I_r, T_c, I_t)$ , some work has proposed using cheaply and automatically generated triplets for training (Gu et al. 2024a; Liu et al. 2024b; Byun et al. 2024). Among these, RTD (Byun et al. 2024) is the most similar to ours, as it fine-tunes the dual encoder using text-only triplets; however, RTD only addresses task discrepancy and is still limited by modality discrepancy. We additionally address modality discrepancy by using triplets that include reference images. Specifically, we employ triplets in

the form of  $(I_r, T_c, T_t)$  for fine-tuning and generate a substantial amount of such triplets on a subset of the publicly available image-caption dataset CC3M (Sharma et al. 2018; Liu et al. 2024a). Detailed information and examples can be found in Appendix.

As illustrated in Figure 3, for image-caption datasets like CC3M (Sharma et al. 2018), each sample consists of an image, denoted as  $I_r$ , and its caption  $T_r$ . The dataset used by MoTaDual is collected through the following process: (1) A powerful LLM, such as Llama (Touvron et al. 2023a,b; Dubey et al. 2024) or GPT-4 (Achiam et al. 2024), is selected, and an effective prompt is designed to instruct the LLM. (2) The caption  $T_r$  in each sample is processed through the LLM using the pre-defined prompt to generate the textual modification  $T_c$  and the target text  $T_t$ . (3) The  $T_c$  and  $T_t$  are merged into the image-caption pair, creating a new triplet dataset for fine-tuning.

# 3.2 Modality-Task Dual Alignment

**Review of CLIP.** Our MoTaDual builds on pre-trained CLIP (Radford et al. 2021; Cherti et al. 2023) model that uses a vast collection of image-caption pairs obtained through web scraping for contrastive training, providing it with powerful cross-modal retrieval capabilities. For text encoding, given an input sequence of words, CLIP first applies byte pair encoding (BPE) (Shin et al. 2020) to convert the words into tokens. In addition, [SOS] and [EOS] are added at the beginning and end of the sequence as special tokens, respectively, and the token sequence is padded to a fixed length. Afterwards, the resulting sequence is mapped to fixed-dimensional embedding vectors and fed into the text encoder  $\mathcal{T}(\cdot)$ , which is a Transformer (Vaswani et al. 2017) consisting of L encoder layers. The embeddings input to the  $(i+1)^{th}$  layer of the transformer is denoted as

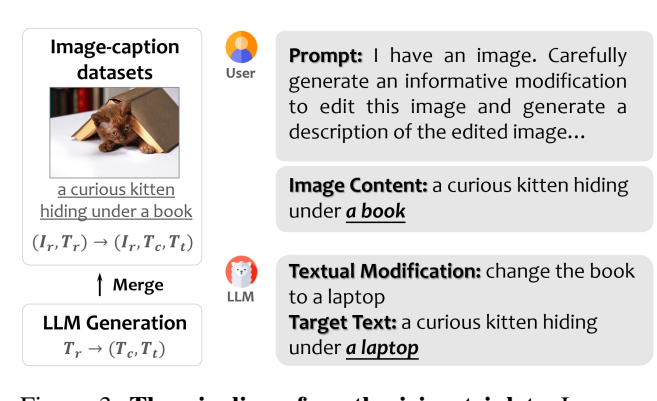


Figure 3: **The pipeline of synthesizing triplets.** Leveraging the strong reasoning abilities of LLMs, an image-caption dataset can be easily transformed into a triplet dataset.

 $W_i = [w_i^1, w_i^2, ..., w_i^N] \in \mathbb{R}^{N \times d}$ , and the equation held by the layer is as follows

$$[W_{i+1}] = \mathcal{T}_{i+1}(W_i) \quad i = 1, 2, \dots, L.$$
 (1)

The outputs from the final layer of the Transformer are projected, and the representation corresponding to the  $N^{th}$  token, i.e. [EOS], is taken as the text feature  $f_t$ .

On the image side, CLIP follows a similar process. An input image is first split into patches by convolution, resulting in a token sequence of length M. These patches are then projected into fixed-dimensional embeddings, denoted as E, and a trainable vector x, namely the [CLS] token, is added. The resulting sequence is subsequently fed into the image encoder  $\mathcal{I}(\cdot)$ , which is a Vision Transformer (ViT) (Dosovitskiy et al. 2021) with depth K. For the input to the  $(i+1)^{th}$  layer, as shown below

$$[x_{i+1}, E_{i+1}] = \mathcal{I}_{i+1}([x_i, E_i]) \quad i = 1, 2, \dots, K.$$
 (2)

Symmetrically to the text branch, the final outputs of the Vision Transformer are projected, and the representation of the <code>[CLS]</code> token serves as the image feature  $f_v$ .

For text-to-image zero-shot inference, the image features  $\mathcal{S}:=\{f_v^i\}_{i=1}^l$  of a specific gallery are pre-extracted by the image encoder. Given a text feature  $f_t$  for a caption, the cosine similarity between  $f_t$  and each image feature  $f_v^k$  in  $\mathcal{S}$  is computed, which is then converted into the probability

$$p(f_v^k|f_t) = \frac{\exp(sim(f_t, f_v^k)/\tau)}{\sum_{i=1}^{l} \exp(sim(f_t, f_v^i)/\tau)}.$$
 (3)

Finally, the image(s) with high probabilities are selected as the retrieval results.

**Incorporating Prompt Tuning to CIR.** Based upon the previously generated triplet data, the dual encoder is fine-tuned. Since the generated triplets involve the image modality, full fine-tuning of the dual encoder would be highly resource-intensive and could lead to catastrophic forgetting (Kemker et al. 2018). Alternatively, MoTaDual employs multi-modal prompt tuning, which preserves the original knowledge while adapting the dual encoder to the CIR task. Prompt tuning involves learning context prompts, which are trainable tokens. In the text side, MoTaDual integrates n

such learnable tokens  $P:=\{p^i\in\mathbb{R}^d\}_{i=1}^n$  with other tokens to serve as input to the text encoder. The input and output of the  $(i+1)^{th}$  layer now adhere to the following equation, where  $[\cdot,\cdot]$  denotes the concatenation operation

$$[P_{i+1}, W_{i+1}] = \mathcal{T}_{i+1}([P_i, W_i]). \tag{4}$$

Meanwhile, a coupling function  $\mathcal{F}$  (a simple linear layer) transfers the context prompts from the language branch to the vision branch of CLIP

$$\tilde{P} = \{ \mathcal{F}(p^i) \in \mathbb{R}^d \}_{i=1}^n. \tag{5}$$

They are then appended to the token sequence on the vision branch before being input into the image encoder. Consequently, the equation held by the  $(i+1)^{th}$  layer of the Vision Transformer is as follows

$$[x_{i+1}, E_{i+1}, \tilde{P}_{i+1}] = \mathcal{I}_{i+1}([x_i, E_i, \tilde{P}_i]).$$
 (6)

As presented in Figure 2(ii), the forward propagation of MoTaDual can be summarized in the context of CIR. For an iteration step, the process begins by fetching the current context prompts P and  $\tilde{P}$ . Given a triplet  $(I_r, T_c, T_t)$ , the reference image  $I_r$  is first tokenized. The resulting tokens are concatenated with  $\tilde{P}$  and input to the image encoder, producing the visual feature  $f_v$ , which is then projected to the token embedding space as a special text token <S\*> through the textual inversion network  $\phi$ . The input text takes the form "a photo of <S\*> that  $T_c$ " After tokenization, the textual context prompts P are inserted into the token sequence, and the composed feature  $f_c$  is finally obtained through Equation (4).

Optimization of the dual encoder. Although the LLM-generated  $T_t$  may not perfectly align with the underlying prompt (conditioned on the CLIP model) for  $I_t$ , the ambiguity and diversity of text still allow it to serve as a reasonable target. Given a mini-batch of N triplets, MoTaDual employs the cross-modal projection matching (CMPM) (Zhang and Lu 2018; Jiang and Ye 2023) loss for fine-tuning. After tokenization,  $T_t$  is processed directly by the text encoder without concatenation with context prompts P, resulting in  $\hat{f}_t$ . For each composed feature  $f_c^i$ , a set  $\{(f_c^i, \hat{f}_t^j), y_{i,j}\}_{j=1}^N$  is established, where  $y_{i,j} = 1$  means the matched pair, while  $y_{i,j} = 0$  indicates an unmatched pair. The matching probability  $p_{i,j}$  for each pair is computed by Equation (3), where we further modify  $\tau$  to be a learnable temperature parameter. The loss  $\mathcal{L}_{c2t}$  is then calculated by

$$\mathcal{L}_{c2t} = KL(\mathbf{p}||\mathbf{q}) = \frac{1}{N} \sum_{i=1}^{N} \sum_{j=1}^{N} p_{i,j} \log(\frac{p_{i,j}}{q_{i,j} + \epsilon}), \quad (7)$$

where  $KL(\cdot||\cdot)$  means the KL divergence,  $\epsilon$  is added to avoid numerical problems, and  $q_{i,j} = y_{i,j}/\sum_{k=1}^N y_{i,k}$  represents the true matching probability.  $\mathcal{L}_{t2c}$  can be computed in a similar manner, and the overall objective is as follows

$$\mathcal{L}_{mtda} = \mathcal{L}_{c2t} + \mathcal{L}_{t2c}. \tag{8}$$

# 3.3 Inference

In the inference, the image encoder is utilized to extract features of an image gallery, resulting in  $S := \{f_v^i\}_{i=1}^N$ . After

Method	Tyme	Backbone	Fashion IQ			posed I1 RR	nage Retrie	GeneCIS	
Method	Type	Dackbone	Fasiii	on iQ		KK	CIRCO		Genecis
			R@10	R@50	R@1	R@5	MAP@5	MAP@10	R@1
Pic2Word <sup>†</sup> (Saito et al. 2023)	P	CLIP-G	31.28	51.89	30.41	58.12	5.54	5.59	10.67
SEARLE <sup>†</sup> (Baldrati et al. 2023)	P	CLIP-G	34.81	55.71	34.80	64.07	13.20	13.85	12.87
ContextI2W (Tang et al. 2024)	P	CLIP-L	27.80	48.90	25.60	55.10	-	-	-
KEDs (Suo et al. 2024)	P	CLIP-L	26.80	47.90	26.40	54.80	-	-	_
CompoDiff (Gu et al. 2024a)	-	CLIP-G	39.02	51.71	26.71	55.14	15.33	17.71	15.48
CIReVL (Karthik et al. 2024)	-	CLIP-G	32.19	52.36	34.65	64.29	<u>26.77</u>	<u>27.59</u>	<u>17.40</u>
MTCIR (Chen and Lai 2023)	-	CLIP-L	35.39	57.44	25.52	54.58	10.36	11.63	
Lincir (Gu et al. 2024b)	P	CLIP-L	26.28	46.49	25.04	53.25	12.59	13.58	12.19
+RTD (Byun et al. 2024)	P	CLIP-L	30.24	51.08	26.63	56.17	17.11	18.11	13.18
+MoTaDual (ours)	P	CLIP-L	28.94	49.43	27.28	56.39	20.42	21.62	16.20
Lincir (Gu et al. 2024b)	P	CLIP-G	45.11	65.69	35.25	65.53	19.81	21.01	13.66
+RTD (Byun et al. 2024)	P	CLIP-G	<u>46.21</u>	67.26	<u>36.31</u>	<u>67.47</u>	21.08	22.29	-
+MoTaDual (ours)	P	CLIP-G	46.67	<u>66.97</u>	38.10	68.94	28.36	29.60	18.83

Table 1: **Performance comparison with state-of-the-art methods.** The methods indicated with † do not provide results in the original papers using CLIP-G as the backbone; these are reproduced by Gu et al. The best results are marked in bold, and the second-best results are underlined. "P" and "-" in the Type column represents projection-based/other method.

that, given the input pair  $(I_r,T_c)$ , following the process outlined in Section 3.2, a composed feature  $f_c$  is obtained. The cosine similarity between  $f_c$  and the features in  $\mathcal S$  is computed, and the top-K results with the highest similarity are selected for retrieval output. In a nutshell, MoTaDual is a simple yet effective method that fine-tunes the dual encoder through multi-modal prompt learning. By introducing only a few learnable tokens while keeping the backbone frozen, it effectively alleviates both task and modality discrepancies.

# 4 Experiments

MoTaDual is evaluated on four widely-used datasets, including three standard composed image retrieval benchmarks, as well as one for conditional image similarity.

**Evaluation benchmarks.** FashionIQ (Wu et al. 2021) is designed to simulate a realistic online shopping chat environment, featuring images in fashion domain. It comprises 30,134 triplets derived from 77,684 images. CIRR (Liu et al. 2021) is the first open-domain dataset in CIR, collecting 21,552 real-life images, with human-generated textual modifications. CIRCO (Baldrati et al. 2023) utilizes real-world images from the COCO dataset (Lin et al. 2014) to develop a benchmark tailored for ZS-CIR with multiple ground truths. GeneCIS (Vaze, Carion, and Misra 2023) assesses the ability to adapt to different definitions of visual similarity.

**Evaluation metrics.** Evaluation of the model primarily employs the Rank-K metric, which measures the probability of finding at least one target image within the top-K candidates based on a composed query. Specifically for CIRCO, the mean Average Precision (mAP) is the main criterion. Higher values in Rank-K and mAP indicate better performance.

**Implementation details.** In the triplets generation procedure, the LLM model Llama 3 (Dubey et al. 2024) is employed. Over two days, using three RTX 4090 24GB GPUs with a batch size of 40, we process approximately 400k sam-

ples from CC3M (Sharma et al. 2018; Liu et al. 2024a), yielding the triplet dataset for MoTaDual fine-tuning. The details of the LLM prompt settings and the generated triplet dataset can be found in Appendix. During the pretraining stage, we strictly adhere to the settings outlined in Lincir (Gu et al. 2024b), training textual inversion networks  $\phi$  with a batch size of 512 on one NVIDIA A100 GPU. In the finetuning phase, considering the distribution shifts in the image modality, we adopt different numbers of context prompts according to the target validation sets (4 for FashionIQ, 8 for CIRR, and 20 for CIRCO/GeneCIS). We use CLIP-L (Radford et al. 2021) and CLIP-G1 (Cherti et al. 2023) as the frozen backbones, and the trainable coupling function  $\mathcal{F}$  employs a simple linear layer with its size determined by the backbone. We employ the AdamW optimizer (Loshchilov and Hutter 2019) with a learning rate set at 1e-3, a weight decay of 0.01, and a batch size of 128 (set to 80 for CLIP-G backbone). The model is trained for 2000 steps within one hour on a single NVIDIA A100 GPU. More details and results on various benchmarks can be found in Appendix.

# 4.1 Comparison with State-of-the-Art Methods

The results in Table 1 list the performance of various methods across different datasets. (1) On the CIRR dataset, MoTaDual achieves SOTA performance. Especially using CLIP-G as the backbone, our method significantly exceeds Lincir, i.e. +2.85% in R@1 and +3.41% in R@5. (2) On the CIRCO dataset, MoTaDual surpasses all projection-based methods by a large margin in both MAP@5 and MAP@10 metrics. Notably, compared to Lincir, it achieves improvements of +8.55% and +8.59% respectively when using CLIP-G as the backbone. Additionally, it shows improvements over CIReVL (Karthik et al. 2024), which is a robust

<sup>&</sup>lt;sup>1</sup>https://github.com/mlfoundations/open\_clip

			Comp	5	GeneCIS		CIRCO		
No.	Method	Params	Full Tuning	Text	Image	R@1	R@3	MAP@5	MAP@10
0	Lincir (Baseline)	-				12.19	32.38	12.59	13.58
1	+Full Fine-Funing	441M	$\checkmark$			16.82	38.27	15.85	17.19
2	+Textual Context Prompts	<1M		$\checkmark$		15.39	36.77	18.10	19.20
3	+Visual Context Prompts	<1M			$\checkmark$	15.67	36.59	<u>18.93</u>	<u>20.18</u>
4	+MoTaDual	<1M		<b>√</b>	✓	16.20	37.58	20.42	21.62

Table 2: **Ablation study.** We conduct experiments on GeneCIS and CIRCO based on CLIP-L, measuring the effectiveness of the optimization strategies, including full fine-tuning, only using textual or visual context prompts, and our MoTaDual. The numbers listed in the Params column refer to the **trainable** parameters, where lincir serves as the baseline without fine-tuning.

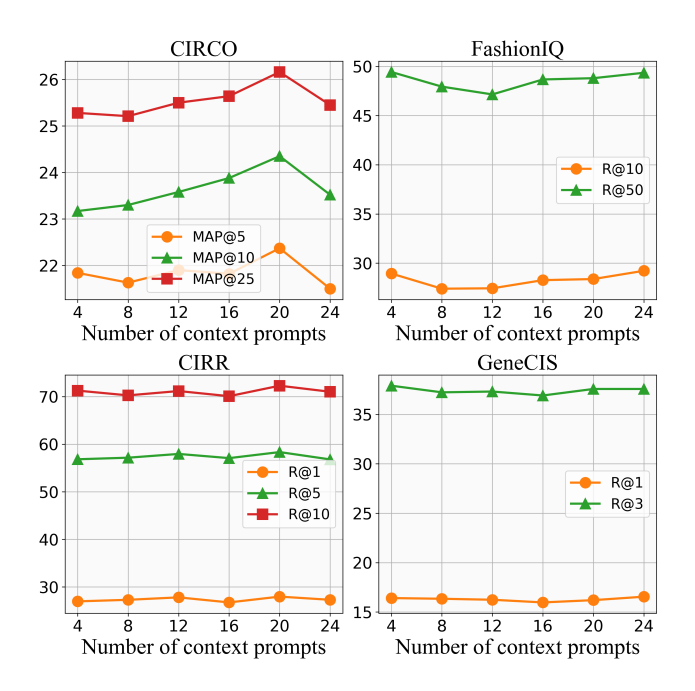


Figure 4: The impact of different numbers of context prompts. We experiment with different numbers of context prompts across four benchmarks.

training-free approach but demands considerable computational resources during inference. This includes generating captions for reference images, reasoning with LLMs, and retrieving target images using the CLIP model. (3) MoTaDual also greatly outperforms other projection-based methods on the GeneCIS benchmark and further exceeds CIReVL, achieving the best results. Based on the CLIP-G backbone. it improves Lincir by +5.17%. (4) For FashionIQ, MoTaDual shows a modest improvement in both R@10 and R@50 over Lincir (Gu et al. 2024b), regardless of the backbone used. The limited gains may be attributed to the fine-tuning triplets being derived from the real-world dataset CC3M, which differs from the fashion-related images and leads to a pronounced domain gap (Wang et al. 2022). Compared to another method based on Lincir, namely RTD (Byun et al. 2024), our approach performs better when using CLIP-G as the backbone but falls short with CLIP-L.

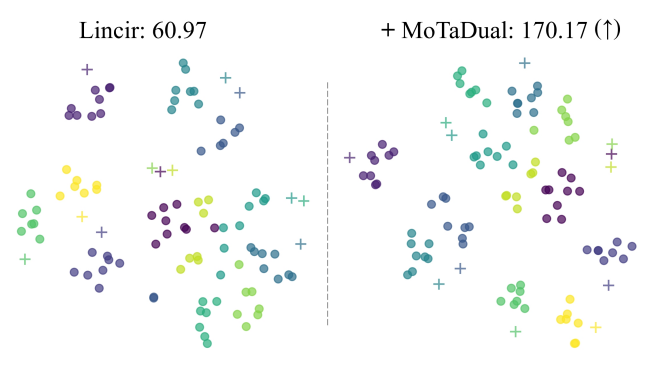


Figure 5: T-SNE (Van der Maaten and Hinton 2008) plots of composed and target features. "+" represents the target image feature, and "o" with the same color denotes the features of its matching bi-modal (image+text) queries.

Methods aimed at eliminating discrepancies. RTD addresses only task discrepancy and relies on full or partial fine-tuning, which is inefficient. Another approach, MT-CIR (Chen and Lai 2023), adopts masked image modeling to simulate the composed image retrieval process. However, due to the information loss and semantic ambiguity, it is not an optimal solution. In contrast, our method is more effective and scalable, substantially enhancing the performance of projection-based approaches by alleviating both task and modality discrepancies, particularly on datasets where these methods typically underperform (CIRCO and GeneCIS).

#### 4.2 Ablation Study

**Optimization Strategies.** We first evaluate the performance of different optimization strategies, as shown in Table 2. The full fine-tuning approach involves substantial computational cost, and it is observed that it can lead to severe distortion and instability. Specifically, since  $\phi$  depends on the dual encoder, any changes in the weights of the dual encoder could cause discrepancies between the features input to  $\phi$  during fine-tuning and those from pre-training. In an extreme case, if  $\phi$  is frozen and only the dual encoder is trained, the performance may drop dramatically. Furthermore, using only textual or visual context prompts already leads to significant improvements over Lincir. In addition, by integrating both types of context prompts, MoTaDual achieves even better re-

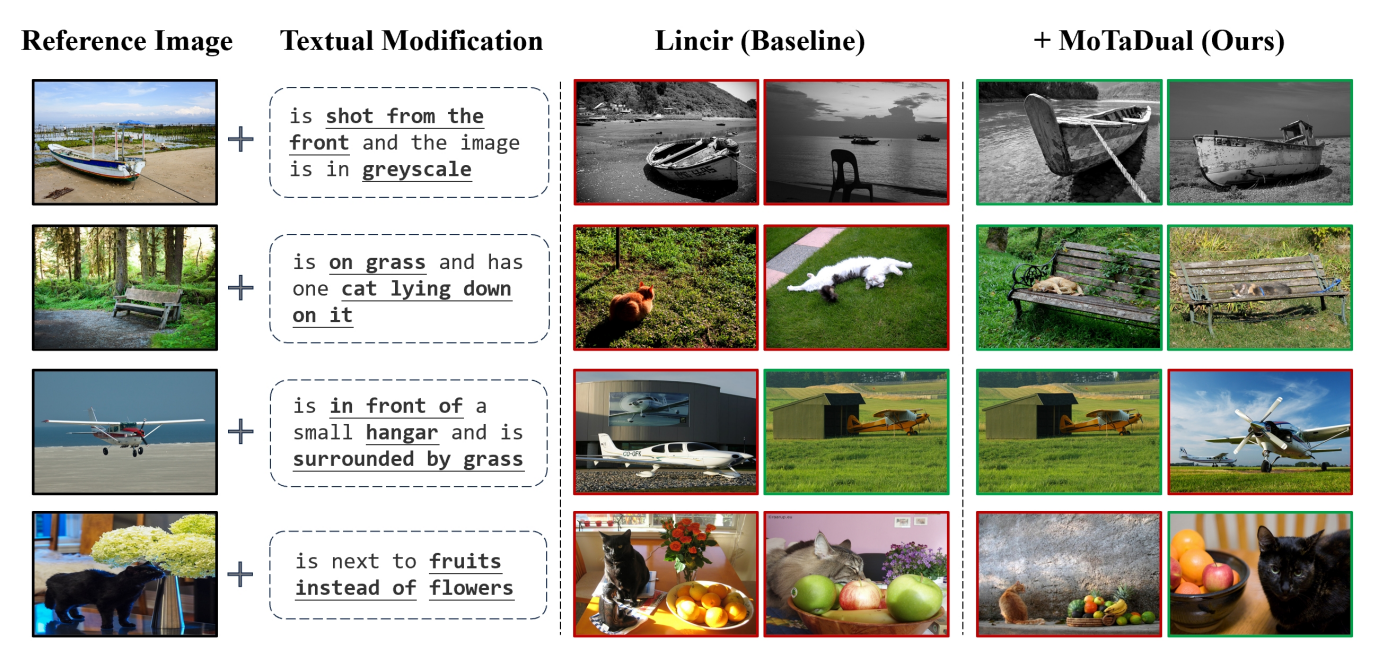


Figure 6: **Qualitative results on CIRCO.** Images with green borders represent ground truth, while those with red borders indicate incorrect predictions.

sults. This underscores the importance of resolving both task and modality discrepancies. Finally, it can also be seen from the table that the amount of trainable parameters in prompt tuning is almost negligible compared to full fine-tuning. This further confirms that MoTaDual is a simple yet effective method, achieving excellent performance while maintaining low computational cost.

Numbers of Context Prompts. Figure 4 shows the impact of different numbers of context prompts. We find that for the real-life datasets, the performance curves are relatively stable and robust, with larger numbers being advantageous. Nevertheless, for FashionIQ, the curve exhibits fluctuations, making it difficult to select an appropriate value. We hypothesize that the difference is due to the real-world images in our generated triplets, which differs from those in FashionIQ but align with the other three benchmarks.

#### 4.3 Qualitative Results

We select the twelve target images with the most matching queries from CIRCO and visualize them using t-SNE (Van der Maaten and Hinton 2008). The results show a significant improvement in clustering after incorporating MoTaDual, with the Calinski-Harabasz index greatly increasing, which indicates that MoTaDual enhances the quality of composed features. Additionally, Figure 6 showcases qualitative predictions by both Lincir and MoTaDual, which further support the effectiveness of our method. MoTaDual is capable of handling fine-grained semantic relationships, such as scene or object composition (row 2-4), in which Lincir fails. Our method also handles domain conversion effectively while performing viewpoint transformation (row 1).

# 5 Analysis

MoTaDual performs the adaptation of both task and modality while preserving the knowledge from the pre-training stage. It requires minimal trainable parameters, demonstrating strong few-shot capabilities and achieving considerable performance gains without the need to fine-tune on the full 400k generated triplet data. Moreover, MoTaDual can easily scale by adjusting the number of context prompts based on the similarity between the fine-tuning dataset and the target dataset, making its application more extensive.

However, there are still some areas for improvement: (1) The textual modifications generated by LLM tend to be repetitive in structure. Therefore, exploring whether supervised fine-tuning (SFT) or other strategies may help to generate more diverse textual modifications is worthwhile. (2) Other Parameter-Efficient Fine-Tuning (PEFT) approaches (Hu et al. 2021; Chen et al. 2022) can also be introduced for further enhancement.

#### 6 Conclusion

In this paper, we present a novel framework for ZS-CIR, which includes two stages: the pre-training stage, where a textual inversion network is trained with only caption data. In the second stage, we propose a new fine-tuning method for ZS-CIR, termed Modality Task Dual Alignment (Mo-TaDual), which leverages triplets generated by LLMs to fine-tune the dual encoder, effectively alleviating both task and modality discrepancies. Notably, owing to the high computational cost of full fine-tuning, we integrate prompt learning into ZS-CIR for the first time, significantly enhancing performance while reducing computational costs. Substantial performance gains on four popular benchmarks demonstrate the effectiveness and superiority of our method.

# References

- Achiam, J.; Adler, S.; Agarwal, S.; Ahmad, L.; Akkaya, I.; Aleman, F. L.; Almeida, D.; Altenschmidt, J.; Altman, S.; Anadkat, S.; et al. 2024. GPT-4 Technical Report. arXiv:2303.08774.
- Anwaar, M. U.; Labintcev, E.; and Kleinsteuber, M. 2021. Compositional learning of image-text query for image retrieval. In *Proceedings of the IEEE/CVF Winter conference on Applications of Computer Vision*, 1140–1149.
- Bahng, H.; Jahanian, A.; Sankaranarayanan, S.; and Isola, P. 2022. Exploring Visual Prompts for Adapting Large-Scale Models. arXiv:2203.17274.
- Baldrati, A.; Agnolucci, L.; Bertini, M.; and Del Bimbo, A. 2023. Zero-shot composed image retrieval with textual inversion. In *Proceedings of the IEEE/CVF International Conference on Computer Vision*, 15338–15347.
- Baldrati, A.; Bertini, M.; Uricchio, T.; and Del Bimbo, A. 2022. Effective conditioned and composed image retrieval combining clip-based features. In *Proceedings of the IEEE/CVF conference on computer vision and pattern recognition*, 21466–21474.
- Byun, J.; Jeong, S.; Kim, W.; Chun, S.; and Moon, T. 2024. Reducing Task Discrepancy of Text Encoders for Zero-Shot Composed Image Retrieval. arXiv:2406.09188.
- Chen, J.; and Lai, H. 2023. Pretrain like Your Inference: Masked Tuning Improves Zero-Shot Composed Image Retrieval. arXiv:2311.07622.
- Chen, S.; Ge, C.; Tong, Z.; Wang, J.; Song, Y.; Wang, J.; and Luo, P. 2022. Adaptformer: Adapting vision transformers for scalable visual recognition. *Advances in Neural Information Processing Systems*, 35: 16664–16678.
- Cherti, M.; Beaumont, R.; Wightman, R.; Wortsman, M.; Ilharco, G.; Gordon, C.; Schuhmann, C.; Schmidt, L.; and Jitsev, J. 2023. Reproducible scaling laws for contrastive language-image learning. In *Proceedings of the IEEE/CVF Conference on Computer Vision and Pattern Recognition*, 2818–2829.
- Cohen, N.; Gal, R.; Meirom, E. A.; Chechik, G.; and Atzmon, Y. 2022. "This is my unicorn, Fluffy": Personalizing frozen vision-language representations. In *European conference on computer vision*, 558–577. Springer.
- Dosovitskiy, A.; Beyer, L.; Kolesnikov, A.; Weissenborn, D.; Zhai, X.; Unterthiner, T.; Dehghani, M.; Minderer, M.; Heigold, G.; Gelly, S.; Uszkoreit, J.; and Houlsby, N. 2021. An Image is Worth 16x16 Words: Transformers for Image Recognition at Scale. arXiv:2010.11929.
- Dubey, A.; Jauhri, A.; Pandey, A.; Kadian, A.; Al-Dahle, A.; Letman, A.; Mathur, A.; Schelten, A.; Yang, A.; Fan, A.; et al. 2024. The Llama 3 Herd of Models. arXiv:2407.21783.
- Fang, K.; Song, J.; Gao, L.; Zeng, P.; Cheng, Z.-Q.; Li, X.; and Shen, H. T. 2024. Pros: Prompting-to-simulate generalized knowledge for universal cross-domain retrieval. In *Proceedings of the IEEE/CVF Conference on Computer Vision and Pattern Recognition*, 17292–17301.

- Gal, R.; Alaluf, Y.; Atzmon, Y.; Patashnik, O.; Bermano, A. H.; Chechik, G.; and Cohen-Or, D. 2022. An Image is Worth One Word: Personalizing Text-to-Image Generation using Textual Inversion. arXiv:2208.01618.
- Gu, G.; Chun, S.; Kim, W.; Jun, H.; Kang, Y.; and Yun, S. 2024a. CompoDiff: Versatile Composed Image Retrieval With Latent Diffusion. arXiv:2303.11916.
- Gu, G.; Chun, S.; Kim, W.; Kang, Y.; and Yun, S. 2024b. Language-only training of zero-shot composed image retrieval. In *Proceedings of the IEEE/CVF Conference on Computer Vision and Pattern Recognition*, 13225–13234.
- He, K.; Zhang, X.; Ren, S.; and Sun, J. 2016. Deep residual learning for image recognition. In *Proceedings of the IEEE conference on computer vision and pattern recognition*, 770–778.
- Hu, E. J.; Shen, Y.; Wallis, P.; Allen-Zhu, Z.; Li, Y.; Wang, S.; Wang, L.; and Chen, W. 2021. LoRA: Low-Rank Adaptation of Large Language Models. arXiv:2106.09685.
- Jia, C.; Yang, Y.; Xia, Y.; Chen, Y.-T.; Parekh, Z.; Pham, H.; Le, Q.; Sung, Y.-H.; Li, Z.; and Duerig, T. 2021. Scaling up visual and vision-language representation learning with noisy text supervision. In *International conference on machine learning*, 4904–4916. PMLR.
- Jia, M.; Tang, L.; Chen, B.-C.; Cardie, C.; Belongie, S.; Hariharan, B.; and Lim, S.-N. 2022. Visual prompt tuning. In *European Conference on Computer Vision*, 709–727. Springer.
- Jiang, D.; and Ye, M. 2023. Cross-modal implicit relation reasoning and aligning for text-to-image person retrieval. In *Proceedings of the IEEE/CVF Conference on Computer Vision and Pattern Recognition*, 2787–2797.
- Karthik, S.; Roth, K.; Mancini, M.; and Akata, Z. 2024. Vision-by-Language for Training-Free Compositional Image Retrieval. arXiv:2310.09291.
- Kemker, R.; McClure, M.; Abitino, A.; Hayes, T.; and Kanan, C. 2018. Measuring catastrophic forgetting in neural networks. In *Proceedings of the AAAI conference on artificial intelligence*, volume 32.
- Khattak, M. U.; Rasheed, H.; Maaz, M.; Khan, S.; and Khan, F. S. 2023. Maple: Multi-modal prompt learning. In *Proceedings of the IEEE/CVF Conference on Computer Vision and Pattern Recognition*, 19113–19122.
- Kim, J.; Yu, Y.; Kim, H.; and Kim, G. 2021. Dual compositional learning in interactive image retrieval. In *Proceedings of the AAAI Conference on Artificial Intelligence*, volume 35, 1771–1779.
- Krishna, R.; Zhu, Y.; Groth, O.; Johnson, J.; Hata, K.; Kravitz, J.; Chen, S.; Kalantidis, Y.; Li, L.-J.; Shamma, D. A.; et al. 2017. Visual genome: Connecting language and vision using crowdsourced dense image annotations. *International journal of computer vision*, 123: 32–73.
- Lester, B.; Al-Rfou, R.; and Constant, N. 2021. The Power of Scale for Parameter-Efficient Prompt Tuning. arXiv:2104.08691.
- Li, J.; Li, D.; Savarese, S.; and Hoi, S. 2023. Blip-2: Bootstrapping language-image pre-training with frozen image

- encoders and large language models. In *International conference on machine learning*, 19730–19742. PMLR.
- Li, J.; Li, D.; Xiong, C.; and Hoi, S. 2022. Blip: Bootstrapping language-image pre-training for unified vision-language understanding and generation. In *International conference on machine learning*, 12888–12900. PMLR.
- Li, J.; Selvaraju, R.; Gotmare, A.; Joty, S.; Xiong, C.; and Hoi, S. C. H. 2021. Align before fuse: Vision and language representation learning with momentum distillation. *Advances in neural information processing systems*, 34: 9694–9705.
- Li, X. L.; and Liang, P. 2021. Prefix-Tuning: Optimizing Continuous Prompts for Generation. In *Proceedings of the 59th Annual Meeting of the Association for Computational Linguistics and the 11th International Joint Conference on Natural Language Processing (Volume 1: Long Papers)*, 4582–4597.
- Lin, T.-Y.; Maire, M.; Belongie, S.; Hays, J.; Perona, P.; Ramanan, D.; Dollár, P.; and Zitnick, C. L. 2014. Microsoft coco: Common objects in context. In *Computer Vision–ECCV 2014: 13th European Conference, Zurich, Switzerland, September 6-12, 2014, Proceedings, Part V 13*, 740–755. Springer.
- Liu, H.; Li, C.; Wu, Q.; and Lee, Y. J. 2024a. Visual instruction tuning. *Advances in neural information processing systems*, 36.
- Liu, Y.; Yao, J.; Zhang, Y.; Wang, Y.; and Xie, W. 2024b. Zero-shot Composed Text-Image Retrieval. arXiv:2306.07272.
- Liu, Z.; Rodriguez-Opazo, C.; Teney, D.; and Gould, S. 2021. Image retrieval on real-life images with pretrained vision-and-language models. In *Proceedings of the IEEE/CVF International Conference on Computer Vision*, 2125–2134.
- Loshchilov, I.; and Hutter, F. 2019. Decoupled Weight Decay Regularization. arXiv:1711.05101.
- Radford, A.; Kim, J. W.; Hallacy, C.; Ramesh, A.; Goh, G.; Agarwal, S.; Sastry, G.; Askell, A.; Mishkin, P.; Clark, J.; et al. 2021. Learning transferable visual models from natural language supervision. In *International conference on machine learning*, 8748–8763. PMLR.
- Russakovsky, O.; Deng, J.; Su, H.; Krause, J.; Satheesh, S.; Ma, S.; Huang, Z.; Karpathy, A.; Khosla, A.; Bernstein, M.; et al. 2015. Imagenet large scale visual recognition challenge. *International journal of computer vision*, 115: 211–252.
- Saito, K.; Sohn, K.; Zhang, X.; Li, C.-L.; Lee, C.-Y.; Saenko, K.; and Pfister, T. 2023. Pic2word: Mapping pictures to words for zero-shot composed image retrieval. In *Proceedings of the IEEE/CVF Conference on Computer Vision and Pattern Recognition*, 19305–19314.
- Schuhmann, C.; Beaumont, R.; Vencu, R.; Gordon, C.; Wightman, R.; Cherti, M.; Coombes, T.; Katta, A.; Mullis, C.; Wortsman, M.; et al. 2022. Laion-5b: An open large-scale dataset for training next generation image-text models. *Advances in Neural Information Processing Systems*, 35: 25278–25294.

- Sharma, P.; Ding, N.; Goodman, S.; and Soricut, R. 2018. Conceptual captions: A cleaned, hypernymed, image alt-text dataset for automatic image captioning. In *Proceedings of the 56th Annual Meeting of the Association for Computational Linguistics (Volume 1: Long Papers)*, 2556–2565.
- Shin, T.; Razeghi, Y.; au2, R. L. L. I.; Wallace, E.; and Singh, S. 2020. AutoPrompt: Eliciting Knowledge from Language Models with Automatically Generated Prompts. arXiv:2010.15980.
- Suhr, A.; Zhou, S.; Zhang, A.; Zhang, I.; Bai, H.; and Artzi, Y. 2019. A Corpus for Reasoning About Natural Language Grounded in Photographs. arXiv:1811.00491.
- Suo, Y.; Ma, F.; Zhu, L.; and Yang, Y. 2024. Knowledge-enhanced dual-stream zero-shot composed image retrieval. In *Proceedings of the IEEE/CVF Conference on Computer Vision and Pattern Recognition*, 26951–26962.
- Tang, Y.; Yu, J.; Gai, K.; Zhuang, J.; Xiong, G.; Hu, Y.; and Wu, Q. 2024. Context-I2W: Mapping Images to Context-dependent Words for Accurate Zero-Shot Composed Image Retrieval. In *Proceedings of the AAAI Conference on Artificial Intelligence*, volume 38, 5180–5188.
- Touvron, H.; Lavril, T.; Izacard, G.; Martinet, X.; Lachaux, M.-A.; Lacroix, T.; Rozière, B.; Goyal, N.; Hambro, E.; Azhar, F.; et al. 2023a. LLaMA: Open and Efficient Foundation Language Models. arXiv:2302.13971.
- Touvron, H.; Martin, L.; Stone, K.; Albert, P.; Almahairi, A.; Babaei, Y.; Bashlykov, N.; Batra, S.; Bhargava, P.; Bhosale, S.; et al. 2023b. Llama 2: Open Foundation and Fine-Tuned Chat Models. arXiv:2307.09288.
- Van der Maaten, L.; and Hinton, G. 2008. Visualizing data using t-SNE. *Journal of machine learning research*, 9(11).
- Vaswani, A.; Shazeer, N.; Parmar, N.; Uszkoreit, J.; Jones, L.; Gomez, A. N.; Kaiser, Ł.; and Polosukhin, I. 2017. Attention is all you need. *Advances in neural information processing systems*, 30.
- Vaze, S.; Carion, N.; and Misra, I. 2023. Genecis: A benchmark for general conditional image similarity. In *Proceedings of the IEEE/CVF Conference on Computer Vision and Pattern Recognition*, 6862–6872.
- Vo, N.; Jiang, L.; Sun, C.; Murphy, K.; Li, L.-J.; Fei-Fei, L.; and Hays, J. 2019. Composing text and image for image retrieval-an empirical odyssey. In *Proceedings of the IEEE/CVF conference on computer vision and pattern recognition*, 6439–6448.
- Wang, J.; Lan, C.; Liu, C.; Ouyang, Y.; Qin, T.; Lu, W.; Chen, Y.; Zeng, W.; and Philip, S. Y. 2022. Generalizing to unseen domains: A survey on domain generalization. *IEEE transactions on knowledge and data engineering*, 35(8): 8052–8072.
- Wu, H.; Gao, Y.; Guo, X.; Al-Halah, Z.; Rennie, S.; Grauman, K.; and Feris, R. 2021. Fashion iq: A new dataset towards retrieving images by natural language feedback. In *Proceedings of the IEEE/CVF Conference on computer vision and pattern recognition*, 11307–11317.
- Xu, X.; Liu, Y.; Khan, S.; Khan, F.; Zuo, W.; Goh, R. S. M.; Feng, C.-M.; et al. 2024. Sentence-level Prompts Benefit

Composed Image Retrieval. In *The Twelfth International Conference on Learning Representations*.

Zhang, Y.; and Lu, H. 2018. Deep cross-modal projection learning for image-text matching. In *Proceedings of the European conference on computer vision (ECCV)*, 686–701.

Zhou, K.; Yang, J.; Loy, C. C.; and Liu, Z. 2022a. Conditional prompt learning for vision-language models. In *Proceedings of the IEEE/CVF conference on computer vision and pattern recognition*, 16816–16825.

Zhou, K.; Yang, J.; Loy, C. C.; and Liu, Z. 2022b. Learning to prompt for vision-language models. *International Journal of Computer Vision*, 130(9): 2337–2348.

# **A** Dataset Details

This part provides a detailed introduction to the four public datasets (Fashion IQ, CIRR, CIRCO and GeneCIS) used in this paper, as well as the triplet datasets generated by LLMs.

# A.1 Benchmarks for ZS-CIR

**Fashion IO** (Wu et al. 2021) is established with the aim of promoting conversational interfaces for online shopping, as a replacement for the traditional keyword-based search interfaces. A key issue that Fashion IQ addresses is interactive fashion image retrieval, which is a standard CIR task, but with the specific focus on fashion-related images. Fashion IO comprises a substantial number of triplets and offers supplementary information, such as product descriptions and visual attribute labels for the fashion images. In Fashion IQ, the samples are categorized into three types: Dress, Shirt, and Toptee. The dataset contains a total of 30,134 triplets derived from 77,684 images. These triplets are split into training, validation, and test sets in a 6:2:2 ratio. Since our approach is designed for ZS-CIR, we do not utilize the training split. Instead, we present results based on the validation set, as shown in Table 5(a). Examples from Fashion IQ are illustrated in Figure 7(a).

CIRR (Liu et al. 2021) is designed to extend CIR to opendomain scenarios, as most CIR benchmarks are confined to a single domain; for instance, Fashion IQ is focused on fashion-related retrieval. CIRR overcomes this limitation by collecting a large number of visually similar images from the real-world dataset, i.e. NLVR (Suhr et al. 2019), using ResNet-152 (He et al. 2016) pre-trained on ImageNet (Russakovsky et al. 2015). Subsequently, the images with high visual similarity are manually annotated to create triplets. The dataset contains a total of 36,554 annotated triplets, which are randomly divided into 8:1:1 for training, validation, and test split. Results on the test split are submitted to a remote server for evaluation. However, CIRR also faces some issues, including unnecessary and ambiguous descriptions in the textual modifications, as well as a lot of false negatives (FNs) that may lead to inaccurate evaluations. We present results on the test split, as shown in Table 5(b). Examples from CIRR are shown in Figure 7(b).

CIRCO (Baldrati et al. 2023) selects a large number of images from the COCO dataset (Lin et al. 2014) for triplet annotation. It is the first CIR benchmark where each query corresponds to multiple ground truths (4.53 on average), which

allows for robust mean average precision (MAP) metrics. CIRCO is specifically designed for ZS-CIR, and therefore does not include a training split. It consists only of a validation split of length 220 and a test split of length 800. Similar to CIRR, results on the CIRCO test split are also submitted to a remote server for validation. Our results on the CIRCO test split are shown in Table 5(c). Examples from CIRCO are demonstrated in Figure 7(c).

GeneCIS (Vaze, Carion, and Misra 2023) evaluates how well models can adapt to a broad set of similarity conditions and is specifically tailored for zero-shot evaluation. GeneCIS comprises four types of conditional retrieval tasks: (1) focus on an object, (2) focus on an attribute, (3) change an object, and (4) change an attribute. Each task within GeneCIS consists of approximately 2,000 queries, with each query having its own gallery set containing 15 samples (10 for "focus on an attribute"). The attribute-based tasks are derived from the VisualGenome (Krishna et al. 2017) dataset, while the object-based tasks are based on the COCO dataset (Lin et al. 2014). Our results on the GeneCIS benchmark are shown in Table 3. Examples from GeneCIS are illustrated in Figure 7(d).

# A.2 Triplet Dataset Generated by LLMs

We selected Llama 3 (Dubey et al. 2024) as the powerful LLM for rewriting image captions to generate textual modifications and target text. Pre-trained weights are provided by the open-source community, HuggingFace<sup>2</sup>, as meta-llama/Meta-Llama-3.1-8B-Instruct. The input prompt is revised from a previous work (Liu et al. 2024b), as shown below.

I have an image. Carefully generate an informative instruction to edit this image and generate a description of the edited image. I will put my image content beginning with "image\_content:". The instruction you generate should begin with "instruction:". The edited description you generate should begin with "edited\_description:". The instruction you generate includes one or two modifications (each with a 50% probability), which can cover various semantic aspects, including cardinality, addition, negation, direct addressing, compare&change, comparative, conjunction, spatial relations&background, viewpoint. Don't just use basic terms like remove, add, or replace in the instruction; try to be a little more diverse. The edited description need to be as simple as possible. The instruction does not need to explicitly indicate which type it is. Avoid adding imaginary things. Each time generate one instruction and one edited description only. The output should be in json format. An example, image\_content: a group of puppies is sitting on a field of dry grass. Your output should strictly follow the format below: {"instruction": "make them sit on the wooden floor with towels", "edited\_description": "some puppies is sitting on a wooden floor covered with towels"}.

Based on the selected LLM, we generate a large amount of triplet data from a filtered subset of CC3M (Liu et al. 2024a), which features a more balanced concept coverage distribution. An example in JSON format is shown below

<sup>&</sup>lt;sup>2</sup>https://huggingface.co

Method	Туре	Backbone	GeneCIS			
	Турс	Buchbone	R@1	R@2	R@3	
Pic2Word <sup>†</sup> (Saito et al. 2023)	P	CLIP-G	10.67	20.70	29.50	
SEARLE <sup>†</sup> (Baldrati et al. 2023)	P	CLIP-G	12.87	22.61	32.46	
CompoDiff (Gu et al. 2024a)	-	CLIP-G	15.48	26.58	35.44	
CIReVL (Karthik et al. 2024)	-	CLIP-G	<u>17.40</u>	<u>29.75</u>	<u>39.48</u>	
Lincir (Gu et al. 2024b)	P	CLIP-L	12.19	22.76	32.38	
+RTD (Byun et al. 2024)	P	CLIP-L	13.18	23.12	32.77	
+MoTaDual (ours)	P	CLIP-L	16.20	27.70	37.58	
Lincir (Gu et al. 2024b)	P	CLIP-G	13.66	24.64	33.54	
+MoTaDual (ours)	P	CLIP-G	18.83	30.36	40.24	

Table 3: **Performance comparison on the general conditional image similarity benchmark GeneCIS.** The methods indicated with † do not provide results in the original papers using CLIP-G as the backbone; these are reproduced by Gu et al. The best results are marked in bold, and the second-best results are underlined. "P" and "-" in the Type column represents projection-based/other method.

Dataset	Optimizer	Batch Size	lr	Warm-up	lr Scheduler	Total Steps	Nctx
Pre-training	AdamW	512	1e-4	-	-	20,000	-
Fashion IQ	AdamW	128	1e-4	100	cosine	500	4
CIRR	AdamW	128	1e-3	100	cosine	500	8
CIRCO	AdamW	128	1e-3	300	cosine	2000	20
GeneCIS	AdamW	128	1e-3	300	cosine	2000	20

Table 4: **Hyperparameter Settings for Modality-Task Dual Alignment.** The number in the warm-up column indicates how many of the total steps are allocated for linear warm-up. "Nctx" represents the number of context prompts.

and some visualization examples from the generated triplet dataset are demonstrated in Figure 8.

The filtered subset of CC3M provides two types of captions: one from the original CC3M dataset, corresponding to the captions of the original images collected from the web, and another generated using BLIP (Li et al. 2022, 2023). Since the web-scraped captions can be quite noisy and may result in lower-quality generated triplets, we adopt the BLIP-generated captions as input for the LLM.

# **B** Full experimental results

**Pre-training textual inversion networks.** We conducted extensive experiments on four ZS-CIR benchmarks. The total process consists of two stages. First is the pre-training stage, where we train separate textual inversion networks for CLIP-L and CLIP-G on large-scale caption datasets. The

key hyperparameters include a batch size of 512, no warm-up phase, and a constant learning rate of 1e-4. The training is performed on a single NVIDIA A100 GPU for a total of 20,000 steps, taking approximately 10 hours for CLIP-G and 3 hours for CLIP-L. Although the pre-training stage is time-consuming, it only needs to be performed once. Afterward, the pre-trained textual inversion networks and the CLIP dual encoder will be frozen, allowing us to focus on Modality-Task Dual Alignment.

Modality-Task Dual Alignment. After completing the pretraining stage and obtaining the corresponding textual inversion networks for different backbones, we move on to the second stage, i.e. MoTaDual, which focuses on adapting the model to the CIR task and addressing the modality discrepancy. For each dataset, we employ dataset-specific hyperparameters to train the context prompts. (1) For Fashion IQ, to fine-tune the dual encoder via prompt learner, we adopt a batch size of 128, a learning rate of 1e-4 with linear warm-up and cosine annealing, and set the number of context prompts to 4. The fine-tuning is conducted for a total of 500 steps on a single NVIDIA A100 GPU, with 100 steps allocated for warm-up. The results for each metric are shown in Table 5(a). (2) For CIRR, the training configuration includes a batch size of 128, a learning rate of 1e-3 with linear warm-up and cosine annealing, and 8 context prompts. The fine-tuning involves a total of 500 steps on a single NVIDIA A100 GPU, with 100 of those steps for warm-up. The detailed results on CIRR are shown in Table 5(b). (3) For CIRCO and GeneCIS, we utilize a batch size of 128 and a learning rate of 1e-3, employing linear warm-up and cosine annealing. The number of context prompts was set to 20. The fine-tuning is conducted for a total of 2000 steps on a single NVIDIA A100 GPU, with 300 steps for warm-up. Detailed experimental results for CIRCO and GeneCIS are presented in Table 5(c) and Table 3, respectively. Due to resource constraints, when using CLIP-G, the batch size is set to 80, while all other parameters remain the same.



(d) GeneCIS examples. The first example shows an example of "Change Object", while the other illustrates an example of "Focus Object".

Figure 7: **Examples of CIR benchmarks.** In all instances, the left side represents the reference image, while the right side is the target image obtained through the given textual modification.

# Reference Image $I_r$

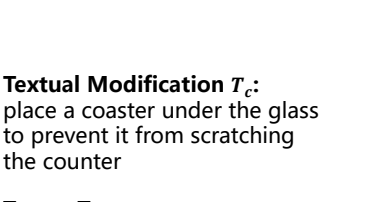


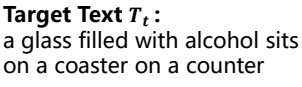
**Textual Modification**  $T_c$ : reorganize the bookshelves to prioritize the favorite books of the children

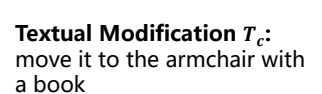
# Target Text $T_t$ : The children's room has a neat arrangement of books, with the favorite books of the kids at eye level



Target Text  $T_t$ : a table is full of lemons and has biscuits on the edges







Target Text  $T_t$ :
A brown teddy bear is sitting on an armchair with a book

# Reference Image $I_r$



**Textual Modification**  $T_c$ : place a bird nearby to catch its attention

Target Text  $T_t$ : a yellow cat is sleeping on a wooden deck with a bird perched nearby



**Textual Modification**  $T_c$ : surround the car with a fence and add some trees in the background

Target Text  $T_t$ : an antique blue car is parked in a fenced lot with some trees in the background



**Textual Modification**  $T_c$ : extend the ramp to meet the stairs

Target Text  $T_t$ : the building has stairs that meet a longer ramp



**Textual Modification**  $T_c$ : swap the drink with a glass of freshly squeezed orange juice

Target Text  $T_t$ : a hamburger is served with a side of fries and a glass of freshly squeezed orange juice

Figure 8: **Examples of triplets generated by the LLM.** The left side is the reference image, and the textual modification and target text are on the right.



Table 5: **Performance comparison on three typical CIR benchmarks.** The methods indicated with † do not provide results in the original papers using CLIP-G as the backbone; these are reproduced by Gu et al. The best results are marked in bold, and the second-best results are underlined. "P" and "-" in the Type column represents projection-based/other method.

(a) Comparison on the FashionIQ validation set.

Method	Туре	Backbone	Shirt		Dress		Toptee		Average	
	Турс	Duckbone	R@10	R@50	R@10	R@50	R@10	R@50	R@10	R@50
Pic2Word <sup>†</sup> (Saito et al. 2023)	P	CLIP-G	33.17	50.39	25.43	47.65	35.24	57.62	31.28	51.89
SEARLE <sup>†</sup> (Baldrati et al. 2023)	P	CLIP-G	36.46	55.35	28.16	50.32	39.83	61.45	34.81	55.71
ContextI2W (Tang et al. 2024)	P	CLIP-L	29.70	48.60	23.10	45.30	30.60	52.90	27.80	48.90
KEDs (Suo et al. 2024)	P	CLIP-L	28.90	48.00	21.70	43.80	29.90	51.90	26.80	47.90
CompoDiff (Gu et al. 2024a)	-	CLIP-G	41.31	55.17	37.78	49.10	44.26	56.41	39.02	51.71
CIReVL (Karthik et al. 2024)	-	CLIP-G	33.71	51.42	27.07	49.53	35.80	56.14	32.19	52.36
MTCIR (Chen and Lai 2023)	-	CLIP-L	38.63	58.51	28.11	51.12	39.42	62.68	35.39	57.44
Lincir (Gu et al. 2024b)	P	CLIP-L	29.10	46.81	20.92	42.44	28.81	50.18	26.28	46.49
+RTD (Byun et al. 2024)	P	CLIP-L	32.83	50.44	24.49	48.24	33.40	54.56	30.24	51.08
+MoTaDual (ours)	P	CLIP-L	32.43	49.85	22.66	45.71	31.72	52.73	28.94	49.43
Lincir (Gu et al. 2024b)	P	CLIP-G	46.76	65.11	38.08	60.88	50.48	71.09	45.11	65.69
+RTD (Byun et al. 2024)	P	CLIP-G	<u>47.20</u>	<u>66.24</u>	<u>39.86</u>	63.01	<u>51.56</u>	72.51	<u>46.21</u>	67.26
+MoTaDual (ours)	P	CLIP-G	47.99	66.78	40.16	<u>62.32</u>	51.86	<u>71.80</u>	46.67	<u>66.97</u>

(b) Comparison on the CIRR test set. R<sub>s</sub>@K measures retrieval performance within a semantically similar subset.

Method	Type	Backbone	CIRR						
	-J P C	2401150110	R@1	R@5	R@10	R <sub>s</sub> @1	R <sub>s</sub> @2	R <sub>s</sub> @3	
Pic2Word <sup>†</sup> (Saito et al. 2023)	P	CLIP-G	30.41	58.12	69.23	68.92	<u>85.45</u>	93.04	
SEARLE <sup>†</sup> (Baldrati et al. 2023)	P	CLIP-G	34.80	64.07	75.11	<u>68.72</u>	84.70	93.23	
ContextI2W (Tang et al. 2024)	P	CLIP-L	25.60	55.10	68.50	-	-	-	
KEDs (Suo et al. 2024)	P	CLIP-L	26.40	54.80	67.20	-	-	-	
CompoDiff (Gu et al. 2024a)	-	CLIP-G	26.71	55.14	74.52	64.54	82.39	91.81	
CIReVL (Karthik et al. 2024)	-	CLIP-G	34.65	64.29	75.06	67.95	84.87	93.21	
MTCIR (Chen and Lai 2023)	-	CLIP-L	25.52	54.58	67.59	55.64	77.54	89.47	
Lincir (Gu et al. 2024b)	P	CLIP-L	25.04	53.25	66.68	57.11	77.37	88.89	
+RTD (Byun et al. 2024)	P	CLIP-L	26.63	56.17	68.96	-	-	-	
+MoTaDual (ours)	P	CLIP-L	27.28	39.13	56.39	58.12	78.05	89.83	
Lincir (Gu et al. 2024b)	P	CLIP-G	35.25	64.72	76.05	63.35	82.22	91.98	
+RTD (Byun et al. 2024)	P	CLIP-G	<u>36.31</u>	67.47	78.31	-	-	-	
+MoTaDual (ours)	P	CLIP-G	38.10	68.94	<b>79.30</b>	68.15	85.59	93.23	

(c) Comparison on the CIRCO test split.

Method	Type	Backbone	CIRCO					
	-JPC	Ducksone	MAP@5	MAP@10	MAP@25	MAP@50		
Pic2Word <sup>†</sup> (Saito et al. 2023)	P	CLIP-G	5.54	5.59	6.68	7.12		
SEARLE <sup>†</sup> (Baldrati et al. 2023)	P	CLIP-G	13.20	13.85	15.32	16.04		
CompoDiff (Gu et al. 2024a)	-	CLIP-G	15.33	17.71	19.45	21.01		
CIReVL (Karthik et al. 2024)	-	CLIP-G	<u>26.77</u>	<u>27.59</u>	<u>29.96</u>	31.03		
MTCIR (Chen and Lai 2023)	-	CLIP-L	10.36	11.63	12.95	13.67		
Lincir (Gu et al. 2024b)	P	CLIP-L	12.59	13.58	15.00	15.85		
+RTD (Byun et al. 2024)	P	CLIP-L	17.11	18.11	20.06	21.01		
+MoTaDual (ours)	P	CLIP-L	20.42	21.62	23.99	25.00		
Lincir (Gu et al. 2024b)	P	CLIP-G	19.71	21.01	23.13	24.18		
+RTD (Byun et al. 2024)	P	CLIP-G	21.08	22.29	24.46	25.44		
+MoTaDual (ours)	P	CLIP-G	28.36	29.60	32.19	33.27		